ELSEVIER

Polymer 43 (2002) 2229–2238

polymer

www.elsevier.com/locate/polymer

Comparative dielectric and TSDC studies of molecular mobility in liquid-crystalline side-chain poly(methacrylate)

N.A. Nikonorova[a,*], T.I. Borisova[a], E.B. Barmatov[b], P. Pissis[c], R. Diaz-Calleja[d]

[a]*Institute of Macromolecular Compounds of Russian Academy of Sciences, Bolshoy pr. 31, 199004 St Petersburg, Russian Federation*
[b]*Moscow State University, 119899 Moscow, Russian Federation*
[c]*Department of Physics, National Technical University of Athens, Zografou Campus, 15780 Athens, Greece*
[d]*Departamento de Termodinamica Aplicada, ETSII, Universidad Politecnica de Valencia, Valencia 4607, Spain*

Received 23 August 2001; accepted 26 November 2001

Abstract

The molecular mobility of a LC side-chain polymethacrylate (PM6) was carried out by dielectric spectroscopy and by thermally stimulated discharge current (TSDC) methods. Six relaxation processes γ_2, γ_1, β, β_1, α, and δ at successively increasing temperatures were observed in PM-6. For each of them, a molecular interpretation was proposed. There is a good correlation between the peak temperature positions obtained from the global TSDC spectrum at an equivalent frequency and those obtained from the dielectric method. The TSDC thermal windowing experiments for PM-6 show the high ability to resolve the overlapping processes at low temperatures. Dielectric and TSDC methods giving different details of the observed relaxation processes, allow us to create the overall picture of molecular mobility in the system under investigation. These two methods revealing the differences and similarities of the obtained results could be considered as complementary to each other. © 2002 Published by Elsevier Science Ltd.

Keywords: LC side-chain polymethacrylate; Dielectric spectroscopy; Thermal windowing experiments

1. Introduction

In experimental studies of dielectric behaviour and molecular mobility of polymers, one is often faced with the problem of resolving two (and more) overlapping processes of relaxation of dipolar polarization. This question is of particular importance for resolving local processes when the more intensive relaxation masks the weaker one. In this case, one broad and non-symmetric peak is typically observed in the frequency or temperature dependence of the dielectric loss factor ε'' or of the dielectric loss tangent tg δ in the range of the overlapping processes [1–3].

In general, the activation energy value defined by the temperature dependence of relaxation time is higher for the process taking place at higher temperature. This means that with decreasing frequency the difference between the relaxation times of these two processes increases.

In addition to the classical dielectric spectroscopy (DS), the method of thermally stimulated discharge currents (TSDC) is also successfully used in the research of dipolar polarization in polymers. The possibility of comparison between the results obtained by the TSDC method and by the dielectric one, is based on the fact that the temperature position of the depolarization current peak T_m correlates with that of ε''_m or tg δ_m peaks observed at the equivalent frequency f_e, which for a local process can be defined by the formula [4,5]:

$$f_e = \frac{E_a r}{2\pi R T_m^2} \tag{1}$$

where E_a is the activation energy of the relaxation process, r the heating rate ($r = dT/dt$), R the gas constant, and T_m the temperature of the discharge current maximum. It follows from Eq. (1) that for $E_a = 10$–60 kcal mol^{-1}, $T_m = 320$ K, and $r = 4$–7 °C min^{-1}, the equivalent frequency is 10^{-3}–10^{-4} Hz. This frequency is lower than that used in DS. It leads to an enhancement of the resolution of different relaxation processes, so that the separation of the peaks on the TSDC curve is better than in the case of the dielectric method.

The TSDC and DS are related techniques, because the origin of the observed peaks is the same, namely, the molecular mobility of polar kinetic units activated by the electric field. These kinetic units during their orientation provide

* Corresponding author. Tel.: +7-812-328-8535; fax: +7-812-328-6869.
E-mail addresses: nikon@imc.macro.ru (N.A. Nikonorova), Cfuceyu2001@email.ru (E.B. Barmatov).

0032-3861/02/$ - see front matter © 2002 Published by Elsevier Science Ltd.
PII: S0032-3861(01)00814-X

contribution to dielectric absorption or to depolarization current. On the other hand, in contrast to DS, the TSDC method is not isothermal. This is its disadvantage. Therefore, it would be interesting to investigate the molecular mobility in polymers by a combination of both TSDC and DS methods and to elucidate the information provided by each of them.

Depending on the way of polarization and thermal treatment, three TSDC techniques can be selected: (1) the TSDC global experiment, (2) the method of partial polarization, and (3) the method of thermal window sampling [4–6].

In the first case, the sample is polarized at a polarization temperature T_p, which is higher than T_g. Then, in the presence of the electric field, the sample is cooled down to T_0 (in practice T_0 is the liquid nitrogen temperature). The field is then removed, the sample is short-circuited and the discharge current is measured and plotted with increasing temperature at a constant rate (4–7 °C min^{-1}) from T_0 to the final temperature $T_f \geq T_p$. As a result, the TSDC global spectrum includes all dielectrically active relaxation processes taking place in the interval from T_0 to T_p.

The method of partial polarization is similar to the first type, but polarization temperatures are selected on the low temperature side of a peak. This means that during partial polarization only one part of dipoles is polarized.

The method of thermal window sampling allows us to reveal the fine structure of the observed processes. With the aid of this technique, the polarization field is applied only in a narrow temperature interval (window). Thus, only a small segment of a global spectrum is polarized. In this technique, the field is applied at T_p (2–5 min), then the sample is cooled (at the presence of a field) down to T_d ($T_d - T_p = 2$–15 °C), and then cooled further, now without a field, down to T_0 ($T_0 - T_p = 10$–20 °C), at which temperature the sample is short-circuited and the discharge current is measured up to T_f ($T_f = T_p + 10$–20 °C). Hence, in this technique the relaxation process is presented by a set of curves with different polarization temperatures.

In the present work, the molecular mobility of a LC side-chain polymethacrylate (PM-6) is investigated. The chemical structure of PM-6 is given below:

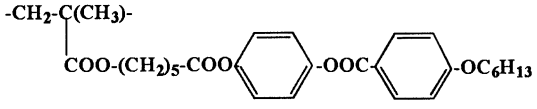

This polymer was obtained at Moscow University in Prof. Shibaev's laboratory. The synthesis of PM-6 has been described in Ref. [7]. The values of the glass transition temperature T_g, the transition temperature from smectic S_X to smectic S_A, and the clearing temperature T_{cl} for PM-6 are 44, 104, and 141 °C, respectively. For comparison, some preliminary measurements obtained with PM-2, where the tail group is $-C_2H_5$ instead of $-C_6H_{13}$ in PM-6 are also shown.

The investigation of PM-6 molecular mobility was carried out by DS and TSDC methods. The purpose of the work is the identification of the various relaxation processes, and also the comparison of the kinetic characteristics of relaxation processes observed by both methods.

2. Experimental part

2.1. Dielectric technique

The frequency dependences of ε' and ε'' at frequencies 10^{-2}–10^6 Hz and temperatures 20–160 °C were measured using a frequency response analyzer (FRA; Schlumberger SI-1260) supplemented by a buffer amplifier of variable gain (Chelsea Dielectric Interface) and an LCR meter (HP 4284A), combined with a TO-19 type thermostatic oven and a SE-70 dielectric cell (ANDO). In addition, the temperature dependences of tg δ were obtained with the aid of a conductivity and capacitance bridge of the TR-9701 type in the temperature range −170– + 150 °C and in the frequency range 60–10^6 Hz. The samples for dielectric measurements were sandwiched at 145 °C (in the isotropic state) between brass electrodes; the diameter of the potential electrode was 20 mm. The sample thickness of 50 μm was maintained by using 50 μm silica fibres.

2.2. TSDC technique

TSDC experiments were curried out with a TSC-RMA (Thermhold) spectrometer on polymer pellets of 0.34 mm thickness and 76 mm^2 surface. In this work, two types of TSDC polarizing techniques were applied: the global experiment ($T_p = 50$ °C for 2 min under a field of 300 V mm^{-1}, $T_0 = -160$ °C, $T_f = 70$ °C, and $r = 7$ °C min^{-1}) and the thermal windowing experiment (poling windows 2 °C, temperature ranges from $T_p - 10$ °C to $T_p + 10$ °C, difference between two successive polarization temperatures 2 or 3 °C, $r = 7$ °C min^{-1}).

3. Results and discussion

3.1. Dielectric investigation

The temperature dependences of tg δ for PM-6 show that in the sub-glass state there are three relaxation processes (Fig. 1).

In the general case, dielectric investigation in the sub-glass state for a great number of thermotropic LC side-chain polyacrylates (PA), polymethacrylates (PMA), and polysiloxanes (PS) with different structures of the mesogens and with different spacer lengths have revealed three local relaxation processes, β, γ_1 and γ_2, at successively decreasing temperatures [8–11].

Successive changes in the chemical structure of side-chain LC polymers (SCLCPs) made it possible to relate

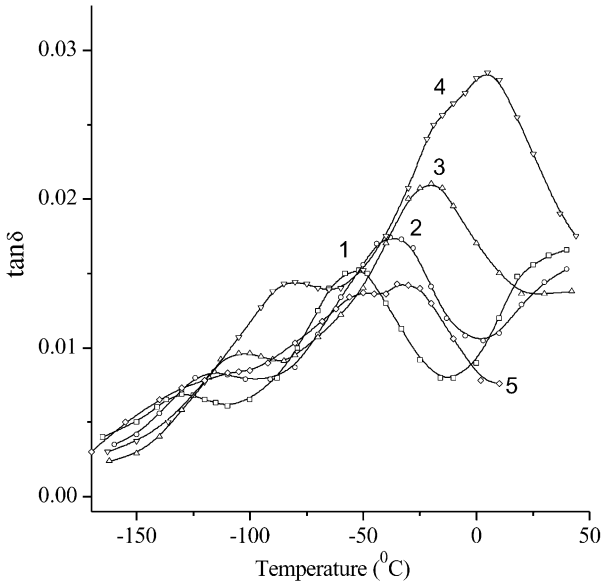

Fig. 1. Temperature dependences of tg δ for PM-6 at 0.1 (1), 1 (2), 10 (3) and 100 kHz (4) and for PM-2 at 1 kHz (5).

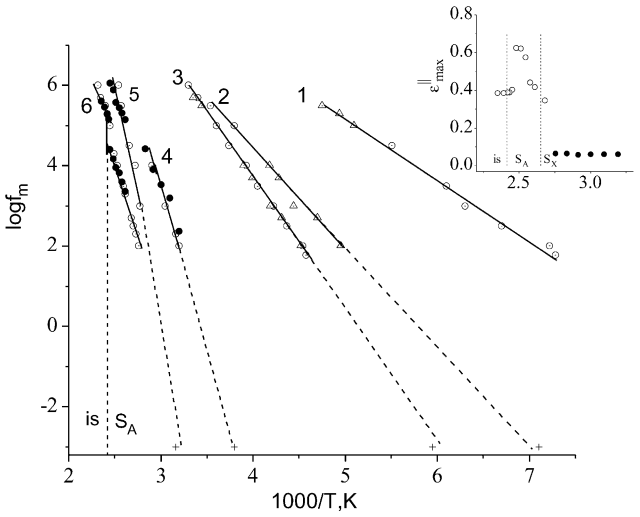

Fig. 2. Dependences of $\log f_m$ on inverse temperature in the ranges of the γ_2 (1), γ_1 (2), β (3), β_1 (4), α (5) δ (6) processes for PM-6 obtained from the tg δ temperature dependences (○), from the ε'' frequency dependences (●) and for PM-2 obtained from the tg δ temperature dependence (△). + — points obtained from the global TSDC curve at equivalent frequency of 10^{-3} Hz. The inset shows the ε''_{max} temperature dependence for the β_1 (●) and δ (○) processes. Dashed lines correspond to the boundaries of the S_X and S_A phases and of the isotropic state.

the β process to the rotational mobility of the mesogen about its long axis. It was shown that the $\log f_m = \varphi(1/T)$ plots in the range of the β process for a great number of SCLCPs are located in a relatively narrow corridor [8]. This means that the conditions of internal rotation of the mesogens in the glassy state depend neither on the spacer length nor on the structure of the main chain and of the mesogen. The activation energies for the β process range from 12 to 18 kcal mol^{-1} [11–13].

The γ_1 process, following the order of temperature and having activation energies of 8–11 kcal mol^{-1}, could be related to the mobility of the methylene spacer. In contrast to the β relaxation, the relaxation times of the γ_1 process for PA-*n* and PMA-*n* (*n* is the number of methylene groups in the spacer) SCLCPs decrease with the methylene spacer length [9]. The difference in relaxation times between β and γ_1 processes decreases with the spacer length reduction. Thus, for PMA-5 and PA-5 SCLCPs with cyanazobenzene and phenynbenzoite mesogen groups, it was possible to observe two overlapping relaxation processes [10]. However, the resolution of the β and γ_1 processes for SCLCPs with $n = 5$ also depends on the relation of the intensities of these processes. For example, it was shown for halogen-containing PMA-5 SCLCPs that a weak γ_1 process is 'hidden' by a much more intensive β process [12]. For PA and PMA SCLCPs with $n = 2$–3, the β and γ_1 processes merge and only one relaxation transition (β/γ_1 process) takes place [10].

The dielectric γ_2 process with activation energies of about 5–8 kcal mol^{-1} reflects the molecular mobility of the polar groups at the end of the mesogen [11–13].

It is reasonable to assume that the three sub-glass processes in Fig. 1 are related to the β, γ_1, and γ_2 processes. One can see that the γ_1 process is revealed only at high frequencies beginning with 100 kHz. This could have two reasons. (1) For PM-6 the spacer length is only five methylene groups. Therefore the difference in the temperature positions of the γ_1 and the β processes is very small. (2) The γ_1 process is hidden by the more intensive β process. For PM-2 it was possible to observe both the β and the γ_1 processes, because their intensities are close to each other (Fig. 1, curve 5). The $\log f_m = \varphi(1/T)$ dependences for the γ_2, γ_1, and β processes, where f_m is the tg δ frequency maximum, are presented in Fig. 2 by curves 1, 2, and 3, respectively. The kinetic units providing the contribution to dielectric absorption in the range of the β and the γ_1 processes are similar for PM-6 and PM-2. In fact, the $\log f_m = \varphi(1/T)$ dependences for both PM-6 and PM-2 in the range of the β process correspond to curve 3 (Fig. 2). One can then assume that the temperature–frequency coordinates of the γ_1 process for PM-6, being very close to those for PM-2, will correspond to curve 2, as in the case of PM-2.

The difference between PM-6 and PM-2 in dielectric behaviour could be expected only for the γ_2 process, because the tail kinetic unit providing the dielectric absorption in this region is much larger in the case of PM-6. However, it was impossible to compare the molecular mobility in the range of the γ_2 process for the two polymers, because in PM-2 the γ_2 process is revealed only as a shoulder on the low temperature side of the γ_1 process.

The values of the activation energies for the β, γ_1 and γ_2 processes, obtained from the slopes of $\log f_m = \varphi(1/T)$ plots in Fig. 2 are 15, 12 and 7 kcal mol^{-1}, respectively.

The temperature dependences of tg δ above room

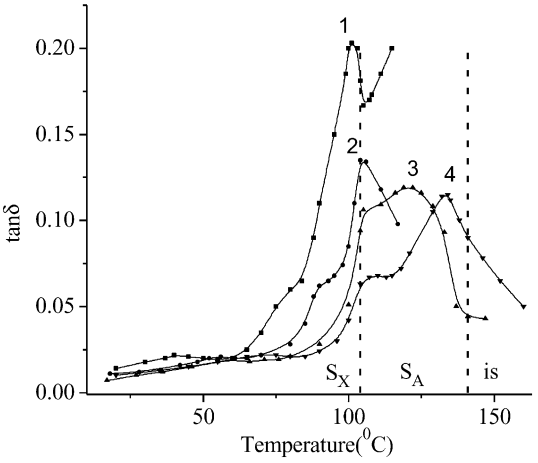

Fig. 3. Temperature dependences of tg δ for PM-6 at 0.1 (1), 1 (2), 10 (3) and 100 kHz (4). Dashed lines correspond to the boundaries of the S_X and S_A phases and of the isotropic state.

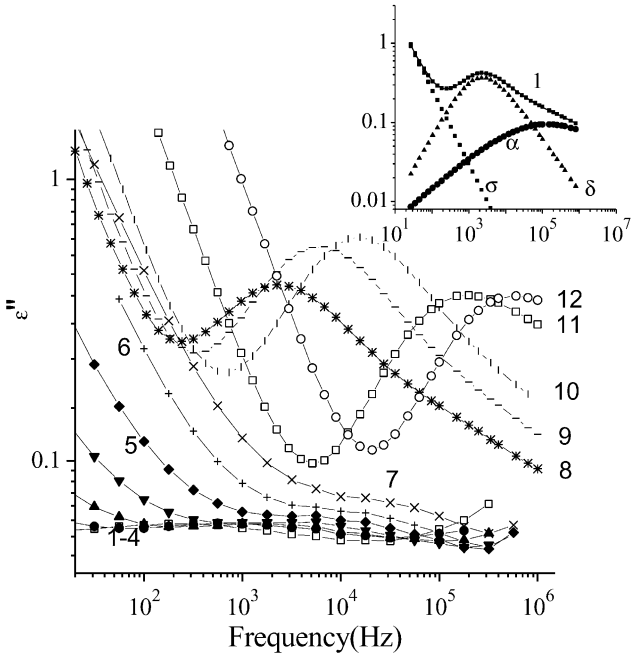

Fig. 4. Frequency dependences of ε'' at: 40 (1), 50 (2), 60 (3), 70 (4), 80 (5), 90 (6), 100 (7), 110 (8), 120 (9), 130 (10), 140 (11), 153 °C (12). The inset shows the same dependence at 110 °C (1), the α and δ processes and the conductivity term σ calculated according to the HN function; the solid line is the fit curve.

temperature show a weak relaxation process around room temperature (which will be denoted as β_1) and two overlapping processes near the glass transition temperature (Fig. 3).

Dielectric studies in SCLCPs show that near T_g two cooperative relaxation transitions (α and δ processes) are observed [8,11,14–18], instead of one relaxation process (α-transition) as in most other polymer classes. The successive change of chemical constitution was allowed to connect the lower temperature relaxation (α process) to the segmental motion, whereas the second relaxation (δ process) may be related to the reorientation of the mesogenic groups. Thus, one can assume that in the case of PM-6, the two relaxation processes near T_g are the α and δ processes.

Fig. 3 shows that the α process is detected only as a shoulder on the low temperature side of the well-defined δ peak. The tg δ_m temperature position for the δ process is well determined to within 0.5–1 °C. For the β_1 and α processes, the tg δ_m temperature positions were determined with accuracy not better than 3–7 °C. This leads to scattering of the points on curves 4 and 5 corresponding to the β_1 and α processes (Fig. 2). The activation energies for the β_1, α, and δ processes, obtained from the slope of curves 4, 5 and 6 in Fig. 2 are 24, 60 and 40 kcal mol^{-1}, respectively.

Although the δ process is the highest temperature relaxation, its activation energy value is lower than that for the α process. The same situation was observed for all thermotropic SCLCPs [10,11,14–16,19]. This can be explained by different molecular mechanisms of these processes. The α process in SCLCPs is very similar to that in polymers of other classes and reflects the segmental mobility of the main chains. The temperature dependence of the relaxation time for the α process could be described by the Vogel–Tammann–Fulcher–Hesse (VTFH) equation [20]. (Only for narrow frequency interval, as in the case of PM-6 in Fig. 2, can the $\log f_m = \varphi(1/T)$ dependence be approximated by a linear curve.) As for the δ process, it takes place only in SCLCPs. The source of this process is the molecular motion of the mesogen group with respect to their short axis. This reorientation needs a large free volume. However, the δ process takes place above T_g in conditions of high molecular mobility of the main chains. As a result, in contrast to the α process, for the δ process the $\log f_m = \varphi(1/T)$ dependence (in the limit of the LC state) can be usually approximated by a linear curve, similar to local processes.

As for the molecular mechanisms of the β_1 process, there are indications that a similar transition was observed only for SCLCPs with the methacrylate main chain [21,22]. It is likely that the origin of the β_1 process is the motion of a kinetic unit including the spacer and the ester group adjoining the main chain. In acrylate SCLCPs, the molecular packing near the main chain is more compact than that in methacrylate polymers, due to the absence of the α-methyl group. That is why in the acrylate systems the motion of the spacer does not include the ester group. It would be useful for the final interpretation of this process to compare the dielectric behaviour of PM-6 with that of PA-6. This will be performed in the future. The intensity of the dielectric absorption of the β_1 process is low, and the beginning of the segmental mobility hides this process. This is the reason why the β_1 process was not observed in all SCLCPs with methacrylate main chain.

For PM-6, the ε'' frequency dependences above room temperature were also measured (Fig. 4). These dependences are less pronounced than the temperature dependences of tg δ in Fig. 3 due to the ε' increase with

Table 1
Havriliak–Negami fit parameters ($\Delta\varepsilon$, α, and β) at different temperatures for the β_1, α, and δ processes obtained from the $\varepsilon'' = \varphi(f)$ dependences in Fig. 4

Relaxation process	T (°C)	$\Delta\varepsilon$	α	β	$\log f_m$
β_1 process	40	0.82	0.55	0.1	2.36
	50	0.84	0.59	0.1	3.21
	60	0.82	0.57	0.1	3.53
	70	0.82	0.61	0.1	3.91
	80	0.78	0.62	0.12	4.42
α process	115	0.55	0.95	0.83	5.32
	120	0.52	0.98	0.92	5.45
	125	0.48	0.98	1	5.58
	130	0.41	0.99	1	5.92
	135	0.40	0.98	0.98	6.01
δ process	115	1.48	1	0.23	3.59
	120	1.55	1	0.25	3.83
	125	1.6	0.96	0.21	3.95
	130	1.6	0.97	0.21	4.17
	135	1.7	0.98	0.27	4.39
	138	1.72	0.98	0.29	5.17
	140	1.75	0.92	0.20	5.28
	145	2.15	0.91	0.21	5.47
	153	2.2	0.91	0.21	5.61

increasing temperature. Comparing the data in Fig. 3, one can assume that the weak peaks of ε'' at low temperatures (40–80 °C) in Fig. 4 are related to the β_1 process, whereas the much more intensive peaks from 110 to 153 °C can be attributed to the two overlapping α and δ processes. In the 85–105 °C range, it was impossible to resolve the weak relaxation process, because it appears only as a shoulder on a high conductivity tail.

The frequency dependences of ε'' in Fig. 4 were described by the Havriliak–Negami (HN) empirical expression [23,24]:

$$[\varepsilon^*(\omega) - \varepsilon_\infty]/[\varepsilon_0 - \varepsilon_\infty] = [1 + (i\omega\tau_0)^{1-\alpha}]^{-\beta} \quad (2)$$

where the parameters α and β $[0 < (1-\alpha), (1-\alpha)\beta \leq 1]$ define the symmetrical and asymmetrical broadening of the loss peak, respectively, τ_0 is the relaxation time, and $f_m = 1/2\pi\tau_0$ is the characteristic frequency at which ε'' passes through the maximum. For the description of the experimental data it was necessary to separate the imaginary and the real parts of Eq. (2) as follows:

$$\varepsilon'(\omega) - \varepsilon_\infty = r^{-\beta/2}(\varepsilon_0 - \varepsilon_\infty)\cos\beta\theta \quad (3a)$$

$$\varepsilon''(\omega) = r^{-\beta/2}(\varepsilon_0 - \varepsilon_\infty)\sin\beta\theta + \frac{A}{\varepsilon_0}\omega^{-s} \quad (3b)$$

where

$$r = \left[1 + (\omega\tau_0^{1-\alpha}\sin\alpha(\pi/2)\right]^2 + \left[(\omega\tau_0)^{1-\alpha}\cos\alpha(\pi/2)\right]^2 \quad (3c)$$

and

$$\theta = \text{arctg}\left[\frac{(\omega\tau_0)^{1-\alpha}\cos\alpha(\pi/2)}{1 + (\omega\tau_0)^{1-\alpha}\sin\alpha(\pi/2)}\right] \quad (3d)$$

The second term in Eq. (3b) for ε'' is the conductivity term, where A is a constant, $s \leq 1$, and ε_0 is the vacuum permittivity [25].

The ε'' frequency dependences in Fig. 4 for the β_1 process and in the range of the α and δ processes were described as one HN process and a conductivity term, or as a sum of two HN processes and a conductivity term, respectively. The HN fit parameters can be seen in Table 1.

Deconvolution of the α and δ processes and the conductivity term at 110 °C is presented as an inset in Fig. 4. The temperature–frequency coordinates of the β_1, α and δ processes obtained from the ε'' frequency dependences in Fig. 4 coincide satisfactorily with curves 4, 5 and 6 in Fig. 2, which were obtained from the tg δ temperature dependences in Fig. 3.

If the δ process takes place both in the LC and in the isotropic state, the $\log f_m = \varphi(1/T)$ dependences have two peculiarities [19,26]. First, the activation energies in the LC state are higher than those in the isotropic state. Second, near T_{cl}, a jump-like decrease (3–8 times) in relaxation time was observed. In the case of PM-6, the $\log f_m = \varphi(1/T)$ dependence for the δ relaxation (curve 6, Fig. 2) includes the transition from the S_A state to the isotropic state. At this transition, there is a jump of about seven times in the relaxation time, and the activation energy changes from 40 in the LC state to 33 kcal mol^{-1} in the isotropic state. This difference is due to the fact that the interaction between mesogens in the LC state exceeds that in the isotropic state. The inset in Fig. 2 shows also that a dramatic change in the intensity of the dielectric absorption ε''_{max} takes place near the temperatures corresponding to (S_X/S_A) and (S_A/isotropic state) transitions. This plot is a good indication of the phase transitions.

3.2. TSDC experiments

The global TSDC spectrum for PM-6 (Fig. 5) shows that in the temperature range from −160 to +70 °C, there are several regions where the depolarization current passes through a maximum: −132, −110, −10, and +43 °C. Postulating that the equivalent frequency of TSDC data is equal to 10^{-3} Hz, the temperature positions of these peaks obtained from the TSDC global spectrum are presented in Fig. 2. Then the curves 2, 3 and 4 (Fig. 2) corresponding to the γ_1, β, and β_1 sub-glass processes were extrapolated to 10^{-3} Hz. This extrapolation shows that the extrapolated temperature positions of the γ_1, β, and β_1 processes at 10^{-3} Hz are very close to the temperature positions of the peaks on the global TSDC curve at −132, −110, and −10, respectively. The γ_2 process has no analogue on the global curve, because the extrapolation of curve 1 in Fig. 2 to 10^{-3} Hz gives −176 °C. This

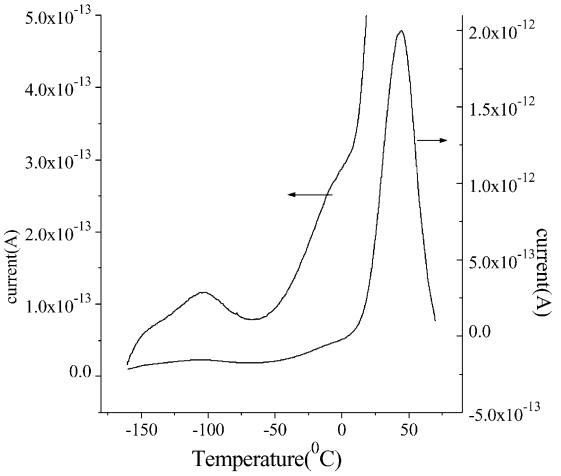

Fig. 5. Global TSDC spectrum for PM-6.

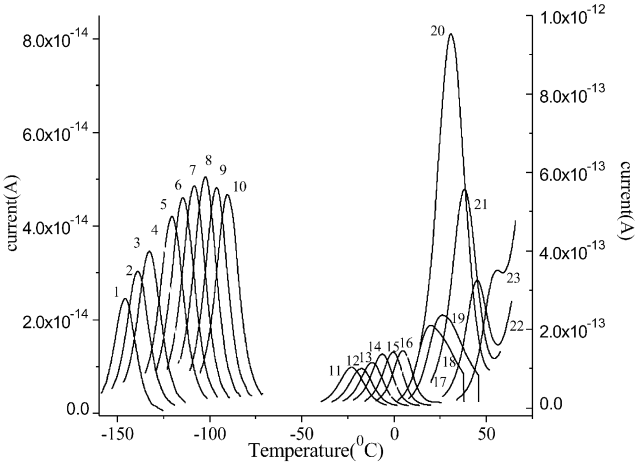

Fig. 6. Set of elementary windowing curves obtained at the poling temperatures −150 (1), −144 (2), −138 (3), −132 (4), −126 (5), −120 (6), −114 (7), −108 (8), −102 (9), −96 (10), −31 (11), −25 (12), −19 (13), −13 (14), −7 (15), −1 (16), 5 (17), 11 (18), 17 (19), 23 (20), 29 (21), 35 (22), 41 °C (23).

temperature is out of the global spectrum range. The main peak on the global curve correlates usually to the α relaxation process. One can see that curve 5 (Fig. 2), corresponding to the α relaxation, extrapolated to 10^{-3} Hz is rather close to 43 °C corresponding to that of the main peak. (However, in this case the linear extrapolation to low frequencies is not correct, because the temperature dependence of relaxation time for the α transition obeys the VTFH equation.) Thus, the results of the overall comparison show that dielectric and TSDC methods are in fairly good agreement.

The thermal windowing TSDC experiments were performed to reveal the details of the processes observed on the global spectrum. These experiments make it possible to activate the narrow fractions or segments of the global peak and to decompose the broad relaxation spectrum into its elementary components with a single relaxation time. The temperature intervals of T_p in the windowing experiments were chosen to cover the region of the β and γ_1 processes (−150 to −80 °C) and the region of the β_1 and α processes (−31 to +45 °C). A series of TSDC thermal windowing experiments are shown in Fig. 6.

In the range of the β and γ_1 processes, the TSDC thermal windowing experiments show that the elementary peaks are rather symmetrical and the shapes of the peaks do not change noticeably in this temperature range (Fig. 6).

In the range of high temperatures, the elementary windowing curves in the temperature interval from −23 to +9 °C (T_p = −31– +5 °C) can be ascribed to the β_1 process (Fig. 6). As for the main TSDC peak, Fig. 6 shows that in the result of the windowing experiments, it was decomposed into two processes. Bearing in mind the dielectric results described in Section 3.1, the first of these processes in the interval from +15 to +39 (T_p = +8– +31 °C) is the α process, whereas the second one in the interval from +43 to +56 °C (T_p = +33– +45 °C) is connected with the beginning of the δ process. (Results of experiments at polarization temperatures higher than +45 °C could not be obtained owing to increasing conductivity contribution.)

For calculating the activation parameters from the windowing experiments, it has been assumed that every elementary cleaning curve could be described by a curve with a single relaxation time, with the temperature dependence given by Ref. [27]:

$$\tau^{-1}(T) = \frac{rJ(T)}{\int_{T_0}^{T} J(T)\mathrm{d}T} \tag{4}$$

where r is the constant heating rate and T_0 is the minimum temperature of the elementary curve. Eq. (4) shows that integration of the elementary TSDC windowing curves allows us to obtain the temperature dependence of relaxation time. The integrated curves obtained from the curves in Fig. 6 are given in Fig. 7.

In the case of Arrhenius (5) or Eyring (6) models, the temperature dependences of relaxation time are expressed by the following equations:

$$\tau(T) = \tau_0(T)\exp\left(\frac{E_a}{kT}\right) \tag{5}$$

$$\tau(T) = \frac{h}{kT}\exp\left(\frac{\Delta G}{kT}\right) \tag{6}$$

$$\Delta G = \Delta H - T_m\,\Delta S \tag{7}$$

where τ_0 is a pre-exponential factor, E_a the activation energy, ΔG the Gibbs free energy, ΔH the enthalpy, ΔS the entropy, and T_m is the temperature of maximum intensity of the elementary peak. The linear part of the integrated curves in Fig. 7 in the interval from (T_p − 2 °C) to (T_p + 2 °C) was chosen for calculating E_a, τ_0, ΔG, ΔH,

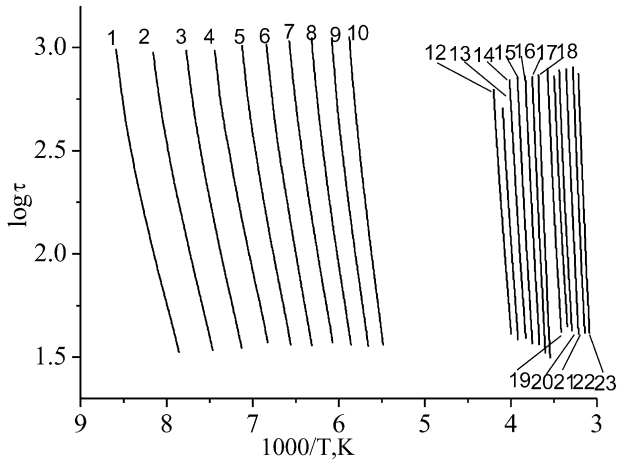

Fig. 7. Arrhenius plots obtained by integration of the elementary windowing curves in Fig. 6 at the poling temperatures −150 (1), −144 (2), −138 (3), −132 (4), −126 (5), −120 (6), −114 (7), −108 (8), −102 (9), −96 (10), −31 (11), −25 (12), −19 (13), −13 (14), −7 (15), −1 (16), 5 (17), 11 (18), 17 (19), 23 (20), 29 (21), 35 (22), 41 °C (23).

and ΔS for every T_p. The results of calculations are presented in Table 2.

For a great number of polymer systems the thermal windowing experiments show that there is a linear dependence between ΔG of different elementary windowing curves and T_m

$$\Delta G = \alpha T_m \tag{8}$$

with α equal to 67 cal K^{-1} mol^{-1} [28,29]. Fig. 8 shows the $\Delta G = \varphi(T_m)$ dependence obtained from the thermal windowing experiments for PM-6. As it was to be expected, our experimental points are on the dashed line corresponding to the slope equal to 67 cal K^{-1} mol^{-1}. Fig. 8 illustrates well that the Gibbs free energy depends only on temperature and is independent of the polymer structure. Moreover, this dependence is valid for all relaxation mechanisms including cooperative processes near the α transition and local processes (β and γ_1) in the glassy state.

Taking into account Eqs. (7) and (8), the entropy factor can be written as

$$\Delta S = \Delta H/T_m - \alpha \tag{9}$$

Eq. (9) indicates that there is a linear relationship between ΔS and $\Delta H/T_m$ with the slope equal to 1 and with the intercept equal to α. The $\Delta S = \varphi(\Delta H/T_m)$ dependence for PM-6 (inset in Fig. 8) shows that for all relaxation processes the experimental points fall on one curve, in agreement with Eq. (9). This means that the ΔS and ΔH values are mutually connected. The $\Delta S = \varphi(\Delta H/T_m)$ and $\Delta G = \varphi(T_m)$ relationships can be considered as calibration curves, because it is sufficient to know only one parameter in order to determine the other one.

Fig. 9 presents dependences ΔG, E_a, and τ_0 versus T_p (ΔS and ΔH plots, repeating those of E_a are not shown). The $\Delta G = \varphi(T_p)$ dependence is linear, as in the case of the $\Delta G = \varphi(T_m)$ dependence, because for PM-6 a linear relationship exists between T_p and T_m (Table 2).

At low temperatures, curves 2 and 3 for E_a and τ_0 show a change of slope (a knee) at a temperature of about −125 °C. This change should be related to the transition from the γ_1 to the β process. For the γ_1 process, the τ_0 and E_a values, equal to 10^{-12} s and 8–10 kcal mol^{-1} are

Table 2
Polarization temperature T_p (°C), temperature of maximum intensity of elementary curve T_m (°C), enthalpy ΔH (kcal mol^{-1}), entropy ΔS (cal K^{-1} mol^{-1}), free Gibbs energy ΔG (kcal mol^{-1}), pre-exponential factor τ_0 (s), and activation energy E_a (kcal mol^{-1}) calculated from elementary windowing experiments

T_p	T_m	ΔH	ΔS	ΔG	log τ_0	E_a
−150	−145	7.62	−3.83	8.09	−12.0	7.83
−144	−139	8.16	−3.06	8.56	−12.3	8.48
−138	−133	8.62	−2.59	8.97	−12.3	8.85
−132	−126	9.05	−2.49	9.40	−12.4	9.31
−126	−120	9.86	0.305	9.82	−13.2	10.3
−123	−117	10.4	2.78	10.0	−13.5	10.7
−120	−115	11.0	4.96	10.2	−14.2	11.4
−117	−112	11.5	6.93	10.4	−14.5	11.8
−114	−109	12.0	8.42	10.6	−14.8	12.2
−111	−106	12.7	11.3	10.8	−15.4	13.0
−108	−103	13.0	12.0	11.0	−15.6	13.3
−105	−99.0	13.6	14.0	11.3	−16.1	13.9
−102	−96.0	14.3	16.4	11.5	−16.6	14.6
−99	−94.0	14.9	18.6	11.7	−17.0	15.2
−96	−90.0	15.7	21.7	11.9	−17.7	16.0
−93	−87.0	16.2	22.7	12.1	−18.0	16.5
−31	−23.1	26.6	43.1	16.6	−22.9	27.0
−28	−20.8	27.9	45.3	16.8	−23.0	28.3
−25	−17.8	28.4	45.8	17.0	−23.2	28.8
−22	−14.9	28.8	46.4	17.2	−23.3	29.3
−19	−12.0	30.0	49.1	17.4	−23.9	30.3
−16	−9.18	30.6	50.5	17.6	−24.2	31.0
−13	−6.70	31.9	54.4	17.7	−25.1	32.3
−10	−3.41	33.3	58.2	18.0	−25.8	33.7
−7	−0.544	35.6	65.3	18.2	−27.6	36.2
−4	2.18	37.3	70.3	18.4	−28.6	37.8
−1	4.74	39.4	75.6	18.5	−29.9	39.8
2	8.47	40.5	78.8	18.8	−30.3	40.8
5	9.19	41.7	82.6	18.9	−31.1	41.9
8	15.2	38.9	69.4	19.3	−28.4	39.3
11	19.8	39.3	69.1	19.7	−28.3	39.8
13	22.3	37.3	60.7	19.9	−26.5	37.7
15	22.5	37.8	62.2	19.8	−26.6	38.0
17	26.0	37.5	60.0	20.1	−26.3	38.0
19	25.6	37.7	60.5	20.0	−26.5	38.2
21	28.4	37.6	59.1	20.2	−26.1	38.1
23	30.9	38.1	59.8	20.4	−26.3	38.6
25	33.0	38.5	60.1	20.6	−26.3	38.9
27	35.3	39.0	60.9	20.8	−26.5	39.5
29	38.1	39.8	62.2	21.0	−26.8	40.3
31	39.3	40.1	62.5	21.1	−26.9	40.6
33	42.6	42.0	67.3	21.4	−27.9	42.4
35	45.2	43.5	70.8	21.7	−28.7	43.9
37	46.2	43.4	70.1	21.7	−28.5	43.8
39	49.0	44.9	72.9	21.9	−29.2	45.2
41	50.8	44.9	72.4	22.0	−29.1	45.3
43	53.2	45.5	73.0	22.2	−29.2	45.8
45	56.2	45.6	73.6	22.4	−29.5	45.9

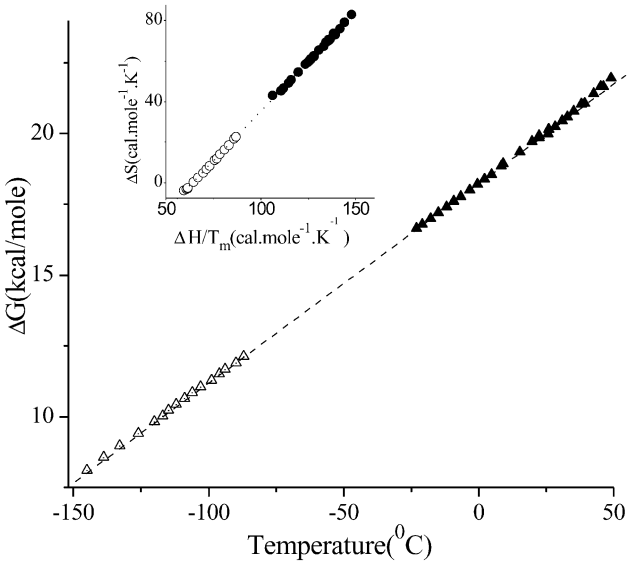

Fig. 8. Gibbs free energy ΔG versus temperature of maximum intensity of elementary peak T_m, dashed line corresponds to the slope equal to 67 cal K^{-1} mol^{-1}. The inset shows the activation entropy ΔS versus $\Delta H/T_m$, dashed line corresponds to the slope equal to 1.

typical of local relaxation processes. Fig. 9 also shows that ΔG and E_a values are similar to each other for the γ_1 process. This means that the $T_m\Delta S$ term in Eq. (7) is equal to zero for the γ_1 process. In the range of the β process, τ_0 changes with temperature from 10^{-12} to 10^{-18} s and E_a increases up to 17 kcal mol^{-1}. This is connected with the molecular mechanism of the β process, because the reorientation of the mesogen about its long axis requires a rather great free volume. For the β process the difference between the E_a and ΔG values increases with T_p, and the entropy factor (although it is small, not more than 3 kcal mol^{-1}) has some importance. The activation energy values obtained from the elementary windowing curves for the γ_1 and β processes are in good agreement with those obtained by the dielectric method.

At high temperatures the dependences of E_a and τ_0 versus T_p (Fig. 9, curves 2 and 3) are much more complicated than those for the low temperature relaxation processes. Similar dependences were observed for LC polymers in Refs. [6,28]. Fig. 9 shows that the plots of E_a and τ_0 versus T_p in the region from -31 to $+5$ °C correspond to the β_1 process. The temperature regions of the α and δ processes are difficult to separate. This could be explained by the following considerations. Although during window experiments only a small part of the global spectrum is polarized, the transitions from the β_1 to the α and from the α to the δ processes cover some temperature intervals. Within this intermediate interval, two processes coexist. Consequently, it is impossible to isolate elementary windowing curves with a single relaxation time. This leads to the scattering points at intermediate temperature ranges. This is probably the reason for the absence of a pronounced transition from the α to δ process in Fig. 9.

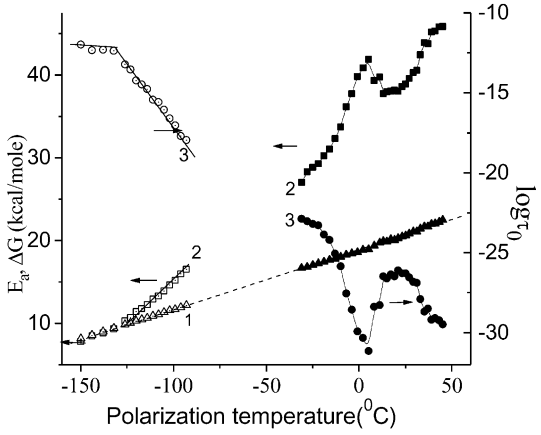

Fig. 9. Gibbs free energy ΔG (1), activation energy E_a (2), and pre-exponential factor τ_0 (3) versus polarization temperature T_p.

3.3. Compensation law

It has been observed that for many thermally stimulated experiments associated with the glass transition the elementary relaxation curves isolated in the complex relaxation mode obey the so-called compensation law [28–32]. Compensation behaviour in polymers is typically observed when E_a, ΔH, ΔS, and log τ_0 values increase concomitantly when the temperature increases. The compensation behaviour has been observed in a large variety of polymeric materials. The compensation point is usually defined by two phenomenological parameters: the compensation temperature, T_c, and the compensation relaxation time, τ_c.

In the framework of the Arrhenius model, the compensation law is expressed as a linear relationship between the logarithm of the pre-exponential factor of the Arrhenius equation and the apparent activation energy [29,33]. Compensation parameters can be determined from the expression

$$\tau_0 = \tau_c \exp(-E_a/RT_c) \quad (10)$$

The substitution of Eq. (10) into the Arrhenius equation $\tau = \tau_0 \exp(E_a/RT)$ gives the following expression:

$$\tau(T) = \tau_c \exp[(E_a(1/T - 1/T_c)/R] \quad (11)$$

According to Eq. (11), the slope of the $\ln(\tau_0) = \varphi(E_a/R)$ dependence determines the reciprocal compensation temperature $(-1/T_c)$, and the intercept determines $\ln \tau_c$. The dependence $\ln(\tau_0) = \varphi(E_a/R)$ for PM-6 in the range of the glass transition (Fig. 10, curve 1) gives the compensation parameters $T_c = 328$ K and $\tau_c = 7.6 \times 10^{-4}$ s.

In the frame of Eyring's theory of activated states, the compensation law can be described in terms of the activation enthalpy–entropy relation $\Delta H_i = T_c\,\Delta S_i + \Delta H_0$, where the variations in the activation enthalpy are compensated for by variations in the activation entropy. If the ΔH and ΔS values increase, there is a linear relationship between ΔS

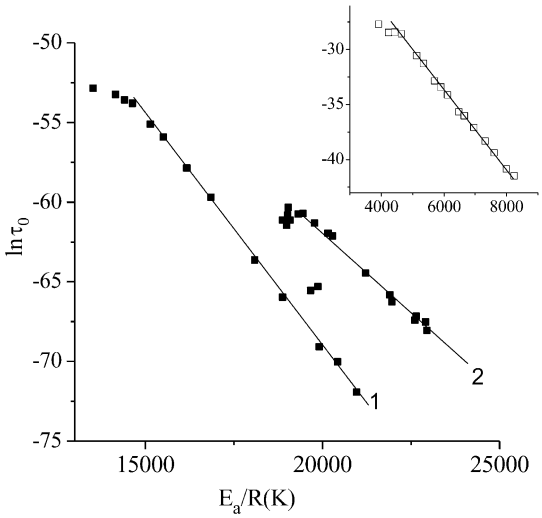

Fig. 10. Logarithm of the pre-exponential factor $\ln \tau_0$ versus activation energy E_a/R for the α (1), β_1 (1), and δ (2) processes. The inset shows the same dependence in the range of the γ_1 and β processes.

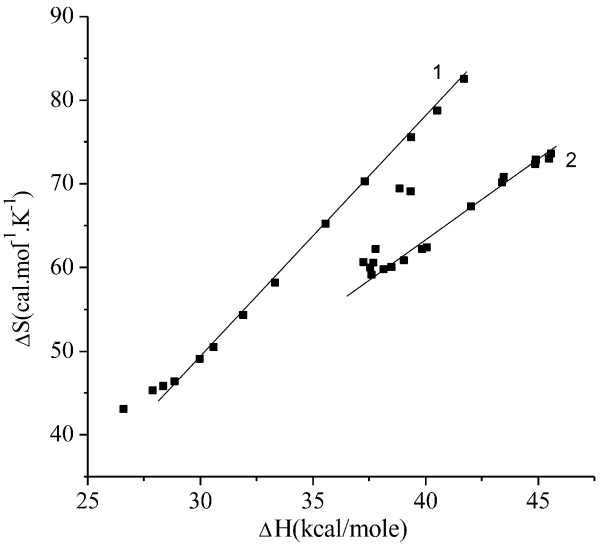

Fig. 11. Activation enthalpy ΔH versus activation entropy ΔS for the α (1), β_1 (1), and δ (2) processes.

and ΔH [28,31]:

$$\Delta S_i = k \ln\left(\frac{h}{kT\tau_c}\right) + \frac{\Delta H_i}{T_c} \quad (12)$$

According to Eq. (12), the compensation temperature can be determined from the slope of the $\Delta S = \varphi(\Delta H)$ dependence. The compensation temperature for PM-6 determined from the $\Delta S = \varphi(\Delta H)$ dependence in the range of the α process (Fig. 11, curve 1) is equal to 331 K. The compensation parameters obtained for the Arrhenius and Eyring models are close to each other within experimental errors.

The glass transition temperature for PM-6 determined by DSC is 44 °C (317 K). This means that the compensation temperature exceeds T_g by 11–14 K. The difference $\Delta T = T_c - T_g$ is usually 5–30 K [30–32,34]. There have been attempts to connect this difference to the stiffness of the polymeric chain. However, detailed comparison of the ΔT with T_g values have not revealed a clear relation between T_c and T_g [30].

Figs. 10 and 11 show that there are two groups of points which are out of the compensation lines related to the glass transition relaxation (curves 1). One group of points (deviations from curves 1 at low E_a, ΔH, and ΔS values) is related to the β_1 process, whereas the second one (curves 2) is related to the δ process. For the latter process, the compensation dependence can also be well approximated by a linear curve and formally the compensation parameters could be calculated from these curves.

The compensation behaviour in polymer systems is often considered as indicative of cooperative segmental molecular movement or some other cooperative transitions due to a sharp increase of activation parameters near T_g. However, if there is an increase of some activation parameter with temperature, the local relaxation processes can also reveal the features of compensation behaviour [30,35]. In the case of PM-6, the dependence of E_a/R versus $\ln \tau_0$ (inset in Fig. 10) is approximated well by a straight line with T_c equal to 275 K. It is not simple to relate this temperature to a temperature characteristic for the specific system under investigation [35].

Until now there is no commonly accepted concept of compensation behaviour but rather a wide spectrum of opinions about this question. One of them is that the compensation law is simply a result of mathematical manipulation and has, therefore, no physical meaning [29]. On the other hand, there have been attempts to relate the compensation parameters to the polymeric properties, for example, to the coefficient of thermal expansion [36] and to T_g [30,37], or to explain the compensation behaviour as an information transfer between the two activation parameters by means of some kind of thermal mechanism [38]. In the latter case, the compensation behaviour is determined by the elements moving with different energy barriers and coupled to a thermal bath with the same coupling function [39]. On the basis of these considerations, the coupling model has also been employed to understand the compensation phenomenon [40]. In spite of different approaches and opinions about the compensation behaviour in polymer systems, the compensation parameters are often used to describe the results of thermal windowing experiments.

4. Conclusions

The dielectric and TSDC techniques were used to study the molecular mobility of a side-chain LC polymethacrylate PM-6. Six relaxations γ_2, γ_1, β, β_1, α, and δ at successively increasing temperatures were observed in PM-6. For every process, a molecular mechanism was proposed. There is a good correlation in the temperature peak positions obtained

from the global TSDC spectrum at the equivalent frequency and in those obtained from the dielectric method. The TSDC thermal windowing experiments showed the high ability to resolve the overlapping processes. For example, in the case of PM-6, the γ_1 and β processes in dielectric studies were recorded as a broad loss peak, whereas by means of TSDC thermal windowing experiments it was possible to separate these two processes.

For the α and δ processes, a different relation of their intensities was observed by the two methods. Thus, in the TSDC experiments the α relaxation is revealed as the main peak, and the δ process of lower intensity can be observed only as a result of thermal windowing experiments. In the dielectric method the inverse situation was observed, since the α process appeared as a shoulder on a much more intensive δ process. This difference may be related to the different natures of the two methods, as the dielectric method is a dynamic one whereas TSDC is static, with the depolarization step (response) being separated from the polarization step (stimulus). Hence, the use of both methods, each of them stressing different aspects and giving different details of the observed relaxation processes, makes it possible to create the overall picture of molecular mobility in the system under investigation. In this sense, the two methods could be considered as complementary to each other. This work revealed the differences and similarities of the results obtained by these two methods.

Acknowledgements

The authors gratefully acknowledge the financial support of University of Valencia and the NATO Science Fellowship Program (Academic Year 2001).

References

[1] Zentel R, Strobl GR, Ringsdorf H. Macromolecules 1985;18:960–5.
[2] Moscicki JK. In: Collyer AA, editor. Liquid crystal polymers: from structure to applications, London: Elsevier, 1992. Chapter 4.
[3] Simon GP. In: Runt JP, Fitzgerald JJ, editors. Dielectric spectroscopy of polymers. Washington, DC: ACS Series, 1997. Chapter 12.
[4] Van Turnhout J. Polym J 1971;2:173–8.
[5] Van Turnhout J. Thermally stimulated discharge of polymer electrets. Amsterdam: Elsevier, 1975.
[6] Mano JF, Correia N, Moura-Ramos JJ, Andrews SR, Williams G. Liq Cryst 1996;20(2):201–17.
[7] Yongjie T. PhD Thesis, Moscow: Moscow State University, 1999.
[8] Borisova TI, Nikonorova NA. Macromol Chem Phys 1998;199: 2147–52.
[9] Nikonorova NA, Borisova TI, Stakhanov AI, Kostromin SG, Shibaev VP. Polym Sci 1998;A40(1):24–9.
[10] Nikonorova NA, Borisova TI, Stakhanov AI, Shibaev VP. Mol Cryst Liq Cryst 1999;331:59–66.
[11] Zhong ZZ, Schuele DE, Gordon WL. Liq Cryst 1994;17(2):199–209.
[12] Nikonorova NA, Borisova TI, Shibaev VP, Barmatov EB, Georgoussis G, Pissis P. Macromol Chem Phys 2001;202:33–8.
[13] Gedde UW, Lui F, Hellermark C, Hult A, Sahlem F, Boyd RH. JMS Pure Appl Chem 1996;A33(10):1555–63.
[14] Attard GS, Williams G, Gray GW, Lacey D, Gemmei PA. Polymer 1986;27(1):185–9.
[15] Araki K. Polym J 1990;22(6):540–50.
[16] Zhong ZZ, Schuele DE, Smith SW, Gordon WL. Macromolecules 1993;26:6403–9.
[17] Parneix JP, Njeumo R, Legrand C, Le Barny P, Dubois JC. Liq Cryst 1987;2(2):167–81.
[18] Nikonorova NA, Borisova TI, Stakhanov AI, Kostromin SG, Shibaev VP. Polym Sci 1999;A41(4):454–60.
[19] Kresse H, Kostromin SG, Shibaev VP. Makromol Chem, Rapid Commun 1982;3:509–13.
[20] Jaeckle J. Rep Prog Phys 1986;49:171–7.
[21] Sanchis MJ, Calleja RD, Gargallo L, Hormazabal A, Radic D. Macromolecules 1999;32(10):3457–63.
[22] Mc Crum NG, Read BE, Williams G. Anelastic and dielectric effects in polymer solids. London: Wiley, 1967. p. 263.
[23] Havriliak S, Negami S. J Polym Sci, Polym Symp 1966;14:99–105.
[24] Havriliak S, Negami S. Polymer 1967;8(1):161–7.
[25] Bottcher CJF, Bordewijk P. Theory of electric polarization. 2nd ed. Amsterdam: Elsevier, 1978. p. 72.
[26] Nikonorova NA, Borisova TI, Shibaev VP. Macromol Chem Phys 2000;201(2):226–32.
[27] Bucci C, Fieschi R. Phys Rev 1964;12(1):1–6.
[28] Ramos JJM, Mano JF, Lacey D, Nestor GJ. Polym Sci, Part B: Polym Phys 1996;34:2067–75.
[29] Sauer BB, Ramos JJM. Polymer 1997;38(16):4065–9.
[30] Ramos JJM, Mano JF, Sauer BB. Polymer 1997;38(5):1081–9.
[31] Teyssedre G, Lacabanne C. Phys D: Appl Phys 1995;28:1478–87.
[32] Doulut S, Bacharan C, Demont P, Bernes A, Lacabanne C. J. Non-Cryst Solids 1998;235–237:645–51.
[33] Shimizu H, Kitano T, Nakayama K. ISE9 1996; p. 552–557.
[34] Lacabanne C, Lamure A, Teyssedre G, Bernes A, Mourgues MJ. Non-Cryst Solids 1994;172:645–51.
[35] Pissis P. J Exp Bot 1990;41(227):677–84.
[36] Sauer BB, Avakian P. Polymer 1992;31:5128–34.
[37] Ibar JP. Thermochim Acta 1991;197:297–333.
[38] Ronarc'h D, Audren P, Moura JL. J Appl Phys 1895;58:474–80.
[39] Peacock-Lopez E, Suhl H. Phys Rev 1982;B26:3774–80.
[40] Ngai KL, Rendell RW, Ragajopal AK, Teiler S. Ann NY Acad Sci 1986;484:150–6.